

# Deep noise squeezing in parametrically driven resonators

Adriano A. Batista<sup>1\*</sup> and Raoni S. N. Moreira<sup>2</sup>, and A. A. Lisboa de Souza<sup>3</sup>

<sup>1</sup>*Departamento de Física, Universidade Federal de Campina Grande*

*Campina Grande-PB, CEP: 58109-970, Brazil*

<sup>2</sup>*Centro de Ciências, Tecnologia e Saúde,*

*Universidade Estadual da Paraíba, Araruna-PB, CEP: 58233000, Brazil*

<sup>3</sup>*Departamento de Engenharia Elétrica, Universidade Federal da Paraíba*

*João Pessoa-PB, CEP: 58.051-970, Brazil*

(Dated: October 1, 2024)

## Abstract

Here we investigate white noise squeezing in the frequency domain of classical parametrically-driven resonators with added noise. We use Green's functions to analyse the response of the resonator to added noise. In one approach, we obtain the Green's function approximately using the first-order averaging method, while in the second approach, exactly, using Floquet theory. We characterize the noise squeezing by calculating the statistical properties of the real and imaginary parts of the Fourier transform of the resonator response to added noise. In the noise spectral density, we observe that the squeezing effects occur only at half the parametric pump frequency. Due to correlation, the squeezing limit of  $-6$  dB can be reached even with detuning at the instability threshold in a single parametrically-driven resonator. We also applied our techniques to investigate squeezing in a system consisting a parametric resonator linearly coupled to a harmonic resonator. In this system, we obtained deep squeezing at around  $-40$  dB in one of the quadratures of the harmonic oscillator response. Finally, we also showed that our analysis of squeezing based on Floquet theory can be applied to multiple coupled resonators with parametric modulation and multiple noise inputs.

---

\* [adriano@df.ufcg.edu.br](mailto:adriano@df.ufcg.edu.br)

## I. INTRODUCTION

Parametric resonators and amplifiers have been implemented in many different systems of physics and engineering such as micro or nanoelectromechanical systems (MEMS/NEMS) [1–3], optomechanics [4], Josephson Junctions [5, 6], atomic force microscopy [7], ion traps [8], etc. Driving parametrically a harmonic resonator is a way to tune its quality factor [9, 10]. A very high effective  $Q$  can thus be obtained. Hence, these amplifiers can achieve very high gains and a very narrow gain bandwidth. The narrow band decreases the effect of fluctuations due to added noise. Further decrease of fluctuations can be achieved when noise squeezing techniques are used. These techniques have been used in high-precision position measurements [11] and also to measure small forces and helped detect gravitational waves in the LIGO experiment [12–14].

In a seminal paper in 1991, Rugar and Grütter [15] experimentally observed thermal noise squeezing of flexural vibrations in a microcantilever. They used a two-phase lock-in amplifier to measure the effect, where the signal was split into two channels in quadrature. The squeezing effect was most noticeable near the transition line of the first parametric instability with the parametric pump frequency set at twice the fundamental mode of the resonator. They predicted a lower bound of  $-6$  dB amplitude deamplification at the parametric instability threshold. They did not propose any theoretical model based on stochastic differential equations to explain this effect.

DiFilippo *et al.* [16] developed noise squeezing techniques for single ion mass spectroscopy based on classical harmonic and anharmonic oscillators parametrically driven at twice the natural frequency only. Their model is based on Hamiltonian time evolution of a Gaussian distribution of initial values, thus neglecting dissipation and noise. They proposed two models of parametric squeezing which they called amplitude (nonlinear squeezing) and quadrature squeezing (around a saddle fixed point). Their model cannot explain the sub-threshold thermomechanical noise squeezing observed experimentally by Rugar and Grütter. In Ref. [17], Cleland investigated thermal noise squeezing in a parametric resonator by analyzing the noise spectral density (NSD) in two channels in quadrature of the slowly-varying variables based on Louisell’s coupled mode method and by making subsequent phase averages over the external ac drive, not via the analysis of stochastic differential equations. Again, the results were limited to resonance when half the pump frequency is equal to the natural frequency of a single-degree-of-freedom parametric resonator.

There have been attempts at increasing thermal noise squeezing beyond the  $-6$  dB level using several different systems and methods such as two-mode coupling in nanomechanical resonators

[18–21], multi-mode coupling [22], feedback [23–25], and nonlinear squeezing [26, 27]. All methods used are approximate solutions adapted to each problem, none of them being general. Instead, what we propose here is a theoretical method that could be applied to all linear parametric amplifier systems without feedback. In addition to that, our method can be applied to nonlinear squeezing if the added noise can be considered as a small perturbation. In nonlinear squeezing, the response to noise will be given by a parametrically driven system in which the pump is given by a stable limit cycle solution of the unperturbed dynamical system (i.e. without added noise) [28]. The only systems that cannot be covered by our present analysis are those with feedback.

We propose a theoretical model based on stochastic differential equations to explain sub-threshold thermal noise squeezing such as first observed by Rugar and Grütter in a classical parametrically driven resonator. In the case of single degree-of-freedom parametrically-driven harmonic oscillators, this behavior is linked to a constraint imposed on the Floquet multipliers by Liouville’s formula. It imposes that the Floquet multipliers can either be a complex conjugate pair with a magnitude less than or equal to 1 or they can be two different real numbers whose product is less than or equal to 1. The squeezing is enhanced when the Floquet exponents are real, leading to two different effective dissipation rates.

We start our theoretical model of noise squeezing analyzing the frequency-domain response of the parametrically modulated resonator to added white noise. The response consists of elastic scattering and parametric up and down conversions. The elastic response is a consequence of the time translation invariant part of the Green’s function. The other responses arise from the non symmetric part of the Green’s function. Subsequently, we split the resonator response into real and imaginary components. Afterwards, we obtain the average fluctuations of the real and imaginary parts and the correlation between them. For a generic pump phase, we obtain these statistical averages from a bivariate Gaussian distribution with correlation. By an appropriate change of coordinates, one can transform from this distribution to a new distribution that is a product of two univariate Gaussian distributions. From the latter distributions, we obtain the length and width of the distribution representing data points obtained in a lockin amplifier (LIA) [15]. Initially, we develop the approximate theory of noise squeezing based on the first-order averaging method and, later, we also develop an exact theory of noise squeezing based on Floquet theory. With this approach we obtained very deep squeezing of fluctuations, near  $-40$  dB, better than any classical result in the literature. This latter approach can be applied to multiple coupled parametrically modulated resonators with added noise.

The remainder of this paper is organized as follows: in Sec. II we state our problem and develop the analytical model of noise squeezing based on the first-order averaging approximation (in Subsec. II A), and on Floquet theory (in Subsec. II B). In Sec. III we present and discuss our results. In Sec. IV we draw our conclusions.

## II. MODEL AND ANALYSIS

In this section, we develop models to explain the phenomenon of classical parametric noise squeezing using two different methods: one using the first-order averaging approximation and the other, exact (in principle) and more general, using Floquet theory.

We initially investigate the effect of added white noise on the single-degree-of-freedom parametrically-driven resonator [29]. Its stochastic differential equation can be written as

$$\ddot{x} = -x - \gamma\dot{x} + F_p \cos(2\omega t + \varphi_p) x + r(t), \quad (1)$$

where  $\gamma$  is the dissipation rate,  $F_p$  is the pump amplitude,  $\omega$  is half the pump frequency,  $\varphi_p$  is the pump phase, and  $r(t)$  is a Gaussian white noise that satisfies the statistical averages  $\langle r(t) \rangle = 0$  and  $\langle r(t)r(t') \rangle = 2D\delta(t - t')$ , where  $D$  is the noise level.

The second model we study is a parametric oscillator coupled to a harmonic oscillator [21]. Its dynamics is given by the following equations of motion

$$\begin{aligned} \ddot{x} &= -\gamma_1\dot{x} - [1 - F_p \sin(2\omega t)]x + \beta_1 y + r_1(t), \\ \ddot{y} &= -\gamma_2\dot{y} - \omega_2^2 y + \beta_2 x + r_2(t), \end{aligned} \quad (2)$$

where  $r_1(t)$  and  $r_2(t)$  are Gaussian white noises that satisfy the statistical averages  $\langle r_1(t) \rangle = \langle r_2(t) \rangle = 0$  and  $\langle r_i(t)r_j(t') \rangle = 2D\delta_{ij}\delta(t - t')$  for  $i, j = 1, 2$ , with  $\delta_{ij} = 1$  if  $i = j$  and 0 otherwise.

The third and most general model we investigate consists of multiple coupled damped parametrically-driven oscillators with added white noise. Its Langevin equation is given by

$$\mathbf{M}\ddot{\mathbf{X}} + \mathbf{\Gamma}\dot{\mathbf{X}} + \mathbf{K}\mathbf{X} = [\mathbf{C}e^{2i\omega t} + \mathbf{C}^*e^{-2i\omega t}] \mathbf{X} + \mathbf{R}(t), \quad (3)$$

where  $\mathbf{X} \in \mathbb{R}^N$ ,  $\mathbf{M}$  and  $\mathbf{\Gamma}$  are positive definite diagonal  $N \times N$  matrices,  $\mathbf{K} \in \mathbb{R}^{N \times N}$  is the elastic coupling  $N \times N$  matrix which is symmetric, and  $\mathbf{C} \in \mathbb{C}^{N \times N}$ . The element  $\mathbf{M}_{ii} = m_i$  is the mass (effective mass) of each resonator (mode). In general, the matrices  $\mathbf{M}$ ,  $\mathbf{\Gamma}$ , and  $\mathbf{K}$  cannot be simultaneously diagonalized. If they can, one could decouple the oscillations into a

superposition of normal modes, turning the problem in a much simpler format, with equations similar to Eq. (2) for each normal mode. In this case, one would necessarily be limited to  $-6$  dB lower limit for squeezing. Here we are interested in the most general case in which the coefficient matrices cannot be diagonalized simultaneously.

#### A. Noise squeezing in the 1st-order averaging approximation

The response in frequency space of the parametrically driven resonator to added white noise [30] is given by

$$\begin{aligned}\tilde{x}(\nu) &= \tilde{G}_0(\nu)\tilde{r}(\nu) - \frac{\beta}{2\omega} \left[ \frac{e^{-i\varphi_p}\tilde{r}(\nu - 2\omega)}{[\rho_- + i(\nu - \omega)][\rho_+ + i(\nu - \omega)]} + \frac{e^{i\varphi_p}\tilde{r}(\nu + 2\omega)}{[\rho_- + i(\nu + \omega)][\rho_+ + i(\nu + \omega)]} \right] \\ &= \tilde{G}_0(\nu)\tilde{r}(\nu) + \Gamma(\nu)\tilde{r}(\nu - 2\omega) + \Gamma^*(-\nu)\tilde{r}(\nu + 2\omega),\end{aligned}\quad (4)$$

where the symbol  $*$  denotes complex conjugation. Here, we use the shorthand notations

$$\Gamma(\nu) = -\frac{\beta}{2\omega} \frac{e^{-i\varphi_p}}{[\rho_- + i(\nu - \omega)][\rho_+ + i(\nu - \omega)]}, \quad (5)$$

$$\tilde{G}_0(\nu) \approx \frac{1}{2\omega} \left[ \frac{\delta + \nu - \omega + i\gamma/2}{[\rho_- + i(\nu - \omega)][\rho_+ + i(\nu - \omega)]} + \frac{\delta - \nu - \omega - i\gamma/2}{[\rho_- + i(\nu + \omega)][\rho_+ + i(\nu + \omega)]} \right], \quad (6)$$

in which  $\rho_{\pm} = -\gamma/2 \pm \kappa$  are the Floquet exponents in the first-order averaging approximation, with  $\kappa = \sqrt{\beta^2 - \delta^2}$ ,  $\beta = -F_p/4\omega$ ,  $\delta = \Omega/2\omega$ , and  $\Omega = 1 - \omega^2$  [31]. Near the onset of instability, at  $\nu = \omega$ , we have

$$\tilde{G}_0(\omega) \approx \frac{1}{2\omega} \left[ \frac{\delta + i\gamma/2}{\rho_- \rho_+} + \frac{\delta - 2\omega - i\gamma/2}{(\rho_- + 2i\omega)(\rho_+ + 2i\omega)} \right] \approx \frac{\delta + i\gamma/2}{2\omega\rho_- \rho_+}. \quad (7)$$

Here, we use the following notation for Fourier transforms

$$\tilde{f}(\nu) = \int_{-\infty}^{\infty} e^{i\nu t} f(t) dt.$$

We are now going to investigate the thermal noise squeezing phenomenon that occurs in the frequency domain of parametrically driven oscillators with added white noise. In order to do that we calculate the real and imaginary parts of  $\tilde{x}(\nu)$ , which we call  $\tilde{x}'$  and  $\tilde{x}''$ , respectively. From Eq. (4), we find

$$\begin{aligned}\tilde{x}'(\nu) &= \tilde{G}'_0(\nu)\tilde{r}'(\nu) - \tilde{G}''_0(\nu)\tilde{r}''(\nu) + \Gamma'(\nu)\tilde{r}'(\nu - 2\omega) - \Gamma''(\nu)\tilde{r}''(\nu - 2\omega) \\ &\quad + \Gamma'(-\nu)\tilde{r}'(\nu + 2\omega) + \Gamma''(-\nu)\tilde{r}''(\nu + 2\omega), \\ \tilde{x}''(\nu) &= \tilde{G}'_0(\nu)\tilde{r}''(\nu) + \tilde{G}''_0(\nu)\tilde{r}'(\nu) + \Gamma'(\nu)\tilde{r}''(\nu - 2\omega) + \Gamma''(\nu)\tilde{r}'(\nu - 2\omega) \\ &\quad + \Gamma'(-\nu)\tilde{r}''(\nu + 2\omega) - \Gamma''(-\nu)\tilde{r}'(\nu + 2\omega),\end{aligned}\quad (8)$$

where the real and imaginary parts of  $\tilde{r}$  are  $\tilde{r}'$  and  $\tilde{r}''$ , respectively. Using the parity properties of the Fourier transform of a real function

$$\begin{aligned}\tilde{r}'(\nu) &= \tilde{r}'(-\nu), \\ \tilde{r}''(\nu) &= -\tilde{r}''(-\nu),\end{aligned}\tag{9}$$

and the following statistical averages of white noise in the frequency domain:

$$\begin{aligned}\langle \tilde{r}'(\nu) \tilde{r}'(\nu') \rangle &= 2\pi D [\delta(\nu - \nu') + \delta(\nu + \nu')], \\ \langle \tilde{r}'(\nu) \tilde{r}''(\nu') \rangle &= 0, \\ \langle \tilde{r}''(\nu) \tilde{r}''(\nu') \rangle &= 2\pi D [\delta(\nu - \nu') - \delta(\nu + \nu')],\end{aligned}\tag{10}$$

we obtain the dispersions in quadrature of the response of the parametric oscillator to added noise, when  $\nu \neq \omega$ . They are given by

$$\begin{aligned}\sigma_c^2(\nu) &= \lim_{\Delta\nu \rightarrow 0^+} \int_{\nu-\Delta\nu}^{\nu+\Delta\nu} \langle \tilde{x}'(\nu) \tilde{x}'(\nu') \rangle d\nu' = 2\pi D \left[ |\tilde{G}_0(\nu)|^2 + |\Gamma(\nu)|^2 + |\Gamma(-\nu)|^2 \right], \\ \sigma_s^2(\nu) &= \lim_{\Delta\nu \rightarrow 0^+} \int_{\nu-\Delta\nu}^{\nu+\Delta\nu} \langle \tilde{x}''(\nu) \tilde{x}''(\nu') \rangle d\nu' = 2\pi D \left[ |\tilde{G}_0(\nu)|^2 + |\Gamma(\nu)|^2 + |\Gamma(-\nu)|^2 \right].\end{aligned}\tag{11}$$

Here,  $\sigma_c$  is the dispersion of the in-phase cosine component and  $\sigma_s$  is the dispersion of the quadrature sine component. We also obtain that there is no correlation between  $\tilde{x}'(\nu)$  and  $\tilde{x}''(\nu)$  when  $\nu \neq \omega$ , that is

$$\lim_{\Delta\nu \rightarrow 0^+} \int_{\nu-\Delta\nu}^{\nu+\Delta\nu} \langle \tilde{x}'(\nu) \tilde{x}''(\nu') \rangle d\nu' = 0.$$

Before we proceed with our theoretical development, we verify that the results we obtain for the NSDs  $S_{\tilde{x}'}$  and  $S_{\tilde{x}''}$  of  $\tilde{x}'$  and  $\tilde{x}''$ , respectively, are consistent with the NSD of  $\tilde{x}$ . That is, we verify below that  $S_{\tilde{x}} = S_{\tilde{x}'} + S_{\tilde{x}''}$  is indeed correct as expected. The NSD  $S_{\tilde{x}}$  is defined [30] as

$$S_{\tilde{x}}(\nu) = \lim_{\Delta\nu \rightarrow 0^+} \int_{\nu-\Delta\nu}^{\nu+\Delta\nu} \frac{\langle \tilde{x}(-\nu) \tilde{x}(\nu') \rangle}{2\pi} d\nu'.\tag{12}$$

With the help of Eq. (4) and Eq. (11), when  $\nu \neq \omega$ , it can be written as

$$S_{\tilde{x}}(\nu) = \frac{\sigma_c^2 + \sigma_s^2}{2\pi} = 2D \left[ |\tilde{G}_0(\nu)|^2 + |\Gamma(\nu)|^2 + |\Gamma(-\nu)|^2 \right].\tag{13}$$

We note that this result is in agreement with the NSD obtained and experimentally confirmed in Ref. [30] in an analog electronic circuit and in a mechanical resonator in Ref. [32]. At  $\nu = \omega$ , we obtain the two dispersions in quadrature and the correlation to be given by

$$\begin{aligned}\sigma_c^2(\omega) &= \lim_{\Delta\nu \rightarrow 0^+} \int_{\omega-\Delta\nu}^{\omega+\Delta\nu} \langle \tilde{x}'(\omega) \tilde{x}'(\nu') \rangle d\nu' \\ &= 2\pi D \left\{ |\tilde{G}_0(\omega)|^2 + |\Gamma(\omega)|^2 + |\Gamma(-\omega)|^2 + 2 \operatorname{Re}\{\tilde{G}_0(\omega)\Gamma(\omega)\} \right\},\end{aligned}\tag{14}$$

$$\begin{aligned}\sigma_s^2(\omega) &= \lim_{\Delta\nu \rightarrow 0^+} \int_{\omega-\Delta\nu}^{\omega+\Delta\nu} \langle \tilde{x}''(\omega) \tilde{x}''(\nu') \rangle d\nu' \\ &= 2\pi D \left\{ |\tilde{G}_0(\omega)|^2 + |\Gamma(\omega)|^2 + |\Gamma(-\omega)|^2 - 2 \operatorname{Re}\{\tilde{G}_0(\omega)\Gamma(\omega)\} \right\},\end{aligned}\quad (15)$$

and

$$\sigma_{cs}(\omega) = \lim_{\Delta\nu \rightarrow 0^+} \int_{\omega-\Delta\nu}^{\omega+\Delta\nu} \langle \tilde{x}'(\omega) \tilde{x}''(\nu') \rangle d\nu' = 4\pi D \operatorname{Im}\left\{\tilde{G}_0(\omega)\Gamma(\omega)\right\}.\quad (16)$$

Experimental data points sampled (with a long enough sample time interval) by a LIA are statistically independent random variates generated by a Gaussian probability distribution with zero mean and these corresponding dispersions and correlation. As the pump amplitude is increased near the instability threshold, the correlation grows giving rise to what is known in the literature as thermal noise squeezing [15]. As  $|\Gamma(-\omega)| \ll |\Gamma(\omega)|$ , we can further simplify these expressions.

More simply, we can write

$$\begin{aligned}\sigma_c^2(\omega) &\approx 2\pi D \left\{ |\tilde{G}_0(\omega)|^2 + |\Gamma(\omega)|^2 - \frac{\beta}{\omega\rho_-\rho_+} \left[ \tilde{G}_0'(\omega) \cos \varphi_p - \tilde{G}_0''(\omega) \sin \varphi_p \right] \right\} \\ &= \frac{\pi D}{2(\omega\rho_-\rho_+)^2} (\delta^2 + \gamma^2/4 + \beta^2 - 2\beta\delta \cos \varphi_p + \beta\gamma \sin \varphi_p) \\ &= \frac{\pi D}{2\omega^2} \frac{\delta^2 + \gamma^2/4 + \beta^2 - 2\beta\delta \cos \varphi_p + \beta\gamma \sin \varphi_p}{(\gamma^2/4 - \kappa^2)^2},\end{aligned}\quad (17)$$

$$\begin{aligned}\sigma_s^2(\omega) &\approx 2\pi D \left\{ |\tilde{G}_0(\omega)|^2 + |\Gamma(\omega)|^2 + \frac{\beta}{\omega\rho_-\rho_+} \left[ \tilde{G}_0'(\omega) \cos \varphi_p - \tilde{G}_0''(\omega) \sin \varphi_p \right] \right\} \\ &= \frac{\pi D}{2(\omega\rho_-\rho_+)^2} (\delta^2 + \gamma^2/4 + \beta^2 + 2\beta\delta \cos \varphi_p - \beta\gamma \sin \varphi_p) \\ &= \frac{\pi D}{2\omega^2} \frac{\delta^2 + \gamma^2/4 + \beta^2 + 2\beta\delta \cos \varphi_p - \beta\gamma \sin \varphi_p}{(\gamma^2/4 - \kappa^2)^2},\end{aligned}\quad (18)$$

$$\sigma_{cs}(\omega) \approx -\frac{\pi D \beta}{\omega^2(\gamma^2/4 - \kappa^2)^2} \left( \frac{\gamma}{2} \cos \varphi_p - \delta \sin \varphi_p \right).\quad (19)$$

Notice that below the instability threshold ( $\beta^2 \leq \gamma^2/4 + \delta^2$ ), one can show that both dispersions are positive. Assuming that  $0 < |\beta| \ll 1$ , we then obtain

$$\sigma_c \sigma_s \approx 2\pi D |\tilde{G}_0(\omega)|^2.\quad (20)$$

For the important special case of  $\delta = 0$  and  $\varphi_p = \pi/2$ , we find

$$\begin{aligned}\sigma_c^2(\omega) &= \frac{\pi D}{2\omega^2} \frac{1}{\left(\frac{\gamma}{2} + \beta\right)^2}, \\ \sigma_s^2(\omega) &= \frac{\pi D}{2\omega^2} \frac{1}{\left(\frac{\gamma}{2} - \beta\right)^2}, \\ \sigma_{cs}(\omega) &= 0.\end{aligned}\quad (21)$$

Further, notice that there is noise squeezing in the dispersions only at  $\nu = \omega$ . With the help of Eq. (16), the noise spectral density at  $\omega$  is given by

$$S_{\tilde{x}}(\omega) = 2D \left[ |\tilde{G}_0(\omega)|^2 + |\Gamma(\omega)|^2 + |\Gamma(-\omega)|^2 \right] \approx \frac{D}{2\omega^2} \frac{\delta^2 + \gamma^2/4 + \beta^2}{(\gamma^2/4 - \kappa^2)^2}. \quad (22)$$

Hence, we see that  $S_{\tilde{x}}(\nu)$  is a continuous function of  $\nu$ , unlike  $\sigma_c(\nu)$  and  $\sigma_s(\nu)$  which present a discontinuous behavior at  $\nu = \omega$ . We believe that the discontinuities at  $\nu = \omega$  of  $\sigma_c(\nu)$  and  $\sigma_s(\nu)$  are due to the fact that we assumed that the noise is completely uncorrelated in time and, consequently, in frequency as well. In reality, when  $\omega$  is very close to  $\omega'$ , one should get  $\langle \tilde{r}(\omega) \tilde{r}(\omega') \rangle \neq 0$ . How close these frequencies have to be so that the correlation is appreciable depends on the physical process that generates the noise  $r(t)$ .

### B. Noise squeezing using Floquet theory

According to Ref. [33], the response in frequency space of the parametrically driven resonator to added white noise is given by

$$\tilde{X}(\nu) \approx \tilde{\mathbf{G}}_0(\nu) \tilde{R}(\nu) + \mathbf{G}_+(\nu) \tilde{R}(\nu - 2\omega) + \mathbf{G}_+^*(-\nu) \tilde{R}(\nu + 2\omega), \quad (23)$$

where  $\tilde{X}$  and  $\tilde{R} \in \mathbb{C}^{2N}$  and the matrices  $\tilde{\mathbf{G}}_0$  and  $\mathbf{G}_+ \in \mathbb{C}^{2N \times 2N}$ . Here, these matrices are given by

$$\begin{aligned} \tilde{\mathbf{G}}_0(\nu) &\approx -p_1^* [B + i(\nu - \omega)I]^{-1} q_1 - p_1 [B + i(\nu + \omega)I]^{-1} q_1^* \\ &= -\sum_k \frac{p_1^* |v_k\rangle \langle v_k| q_1}{\rho_k + i(\nu - \omega)} - \sum_k \frac{p_1 |v_k\rangle \langle v_k| q_1^*}{\rho_k + i(\nu + \omega)}, \\ \mathbf{G}_+(\nu) &= -p_1^* [B + i(\nu - \omega)I]^{-1} q_1^* = -\sum_k \frac{p_1^* |v_k\rangle \langle v_k| q_1^*}{\rho_k + i(\nu - \omega)}. \end{aligned} \quad (24)$$

The vectors  $|v_k\rangle$  are Floquet eigenvectors with corresponding Floquet exponents  $\rho_k$ . Also, note that according to Floquet's theorem, the fundamental matrix of coherent evolution of Eq.(1), i.e. without the added noise, can be written as  $\Phi(t) = P(t)e^{Bt}$ , where  $P(t+T) = P(t)$  is a periodic matrix. Furthermore, we assume that we are near (in parameter space) the first parametric instability region where  $T = \pi/\omega$ . Therefore, we can write the Fourier series expansions of the periodic matrices

$$\begin{aligned} P(t) &= \sum_{n=-\infty}^{\infty} p_n e^{in\omega t}, \\ Q(t) &= \sum_{n=-\infty}^{\infty} q_n e^{in\omega t}, \end{aligned} \quad (25)$$



where  $Q(t) = P^{-1}(t)$ .

### 1. Two-dimensional case

For the case of a single degree-of-freedom parametric oscillator with added noise we have

$$\tilde{x}(\nu) \approx \tilde{\mathcal{G}}_0(\nu)\tilde{r}(\nu) + \mathcal{G}_+(\nu)\tilde{r}(\nu - 2\omega) + \mathcal{G}_+^*(-\nu)\tilde{r}(\nu + 2\omega), \quad (26)$$

where the coefficients  $\tilde{\mathcal{G}}_0(\nu) = \langle 1 | \tilde{\mathbf{G}}_0(\nu) | 2 \rangle$  and  $\mathcal{G}_+(\nu) = \langle 1 | \mathbf{G}_+(\nu) | 2 \rangle$ . Note that in this subsection, we replaced the notation  $\tilde{X}_1$  by  $\tilde{x}$ .

Similarly to Eq. (8), we find

$$\begin{aligned} \tilde{x}'(\nu) &= \tilde{\mathcal{G}}_0'(\nu)\tilde{r}'(\nu) - \tilde{\mathcal{G}}_0''(\nu)\tilde{r}''(\nu) + [\mathcal{G}_+'(\nu)\tilde{r}'(\nu - 2\omega) - \mathcal{G}_+''(\nu)\tilde{r}''(\nu - 2\omega) \\ &\quad + \mathcal{G}_+'(-\nu)\tilde{r}'(\nu + 2\omega) + \mathcal{G}_+''(-\nu)\tilde{r}''(\nu + 2\omega)], \\ \tilde{x}''(\nu) &= \tilde{\mathcal{G}}_0'(\nu)\tilde{r}''(\nu) + \tilde{\mathcal{G}}_0''(\nu)\tilde{r}'(\nu) + [\mathcal{G}_+'(\nu)\tilde{r}''(\nu - 2\omega) + \mathcal{G}_+''(\nu)\tilde{r}'(\nu - 2\omega) \\ &\quad + \mathcal{G}_+'(-\nu)\tilde{r}''(\nu + 2\omega) - \mathcal{G}_+''(-\nu)\tilde{r}'(\nu + 2\omega)]. \end{aligned} \quad (27)$$

Hence, we obtain the dispersions in quadrature of the response of the parametric oscillator to added noise, when  $\nu \neq \omega$ . They are given by

$$\begin{aligned} \sigma_c^2(\nu) &= \lim_{\Delta\nu \rightarrow 0^+} \int_{\nu-\Delta\nu}^{\nu+\Delta\nu} \langle \tilde{x}'(\nu)\tilde{x}'(\nu') \rangle d\nu' = 2\pi D \left\{ |\tilde{\mathcal{G}}_0(\nu)|^2 + |\mathcal{G}_+(\nu)|^2 + |\mathcal{G}_+(-\nu)|^2 \right\}, \\ \sigma_s^2(\nu) &= \lim_{\Delta\nu \rightarrow 0^+} \int_{\nu-\Delta\nu}^{\nu+\Delta\nu} \langle \tilde{x}''(\nu)\tilde{x}''(\nu') \rangle d\nu' = 2\pi D \left\{ |\tilde{\mathcal{G}}_0(\nu)|^2 + |\mathcal{G}_+(\nu)|^2 + |\mathcal{G}_+(-\nu)|^2 \right\}. \end{aligned} \quad (28)$$

We also obtain that there is no correlation between  $\tilde{x}'(\nu)$  and  $\tilde{x}''(\nu)$  when  $\nu \neq \omega$ , that is

$$\lim_{\Delta\nu \rightarrow 0^+} \int_{\nu-\Delta\nu}^{\nu+\Delta\nu} \langle \tilde{x}'(\nu)\tilde{x}''(\nu') \rangle d\nu' = 0.$$

With the help of the definitions of NSD given in Eq. (12) and of Eq. (26), when  $\nu \neq \omega$ ,  $S_{\tilde{x}}$  can be written as

$$S_{\tilde{x}}(\nu) = 2D \left\{ |\tilde{\mathcal{G}}_0(\nu)|^2 + |\mathcal{G}_+(\nu)|^2 + |\mathcal{G}_+(-\nu)|^2 \right\}. \quad (29)$$

When  $\nu = \omega$ , we obtain the two dispersions in quadrature and the correlation to be given by

$$\begin{aligned}\sigma_c^2(\omega) &= \lim_{\Delta\nu \rightarrow 0^+} \int_{\omega-\Delta\nu}^{\omega+\Delta\nu} \langle \tilde{x}'(\omega) \tilde{x}'(\nu') \rangle d\nu' \\ &= 2\pi D \left[ |\tilde{\mathcal{G}}_0(\omega)|^2 + |\mathcal{G}_+(\omega)|^2 + |\mathcal{G}_+(-\omega)|^2 + 2 \operatorname{Re} \left\{ \tilde{\mathcal{G}}_0(\omega) \mathcal{G}_+(\omega) \right\} \right],\end{aligned}\quad (30)$$

$$\begin{aligned}\sigma_s^2(\omega) &= \lim_{\Delta\nu \rightarrow 0^+} \int_{\omega-\Delta\nu}^{\omega+\Delta\nu} \langle \tilde{x}''(\omega) \tilde{x}''(\nu') \rangle d\nu' \\ &= 2\pi D \left[ |\tilde{\mathcal{G}}_0(\omega)|^2 + |\mathcal{G}_+(\omega)|^2 + |\mathcal{G}_+(-\omega)|^2 - 2 \operatorname{Re} \left\{ \tilde{\mathcal{G}}_0(\omega) \mathcal{G}_+(\omega) \right\} \right],\end{aligned}\quad (31)$$

$$\sigma_{cs}(\omega) = \lim_{\Delta\nu \rightarrow 0^+} \int_{\omega-\Delta\nu}^{\omega+\Delta\nu} \langle \tilde{x}'(\omega) \tilde{x}''(\nu') \rangle d\nu' = 4\pi D \operatorname{Im} \left\{ \tilde{\mathcal{G}}_0(\omega) \mathcal{G}_+(\omega) \right\}.\quad (32)$$

## 2. The $2N$ -dimensional case

According to Eq. (23), the response in frequency space of an  $2N$ -dimensional parametrically driven linear dynamical system to added white noise is given by

$$\tilde{X}_i(\nu) \approx \sum_j \left[ \tilde{\mathbf{G}}_{0,ij}(\nu) \tilde{R}_j(\nu) + \mathbf{G}_{+,ij}(\nu) \tilde{R}_j(\nu - 2\omega) + \mathbf{G}_{+,ij}^*(-\nu) \tilde{R}_j(\nu + 2\omega) \right].\quad (33)$$

We point out that from these  $2N$  coordinates  $N$  are position and  $N$  are velocity coordinates. In the notation we use, an odd index points to a position coordinate and an even index points to a velocity coordinate. For this case, we find

$$\begin{aligned}\tilde{X}_i'(\nu) &= \sum_j \left\{ \tilde{\mathbf{G}}'_{0,ij}(\nu) \tilde{R}_j'(\nu) - \tilde{\mathbf{G}}''_{0,ij}(\nu) \tilde{R}_j''(\nu) + \left[ \mathbf{G}'_{+,ij}(\nu) \tilde{R}_j'(\nu - 2\omega) - \mathbf{G}''_{+,ij}(\nu) \tilde{R}_j''(\nu - 2\omega) \right. \right. \\ &\quad \left. \left. + \mathbf{G}'_{+,ij}(-\nu) \tilde{R}_j'(\nu + 2\omega) + \mathbf{G}''_{+,ij}(-\nu) \tilde{R}_j''(\nu + 2\omega) \right] \right\}, \\ \tilde{X}_i''(\nu) &= \sum_j \left\{ \tilde{\mathbf{G}}'_{0,ij}(\nu) \tilde{R}_j''(\nu) + \tilde{\mathbf{G}}''_{0,ij}(\nu) \tilde{R}_j'(\nu) + \left[ \mathbf{G}'_{+,ij}(\nu) \tilde{R}_j''(\nu - 2\omega) + \mathbf{G}''_{+,ij}(\nu) \tilde{R}_j'(\nu - 2\omega) \right. \right. \\ &\quad \left. \left. + \mathbf{G}'_{+,ij}(-\nu) \tilde{R}_j''(\nu + 2\omega) - \mathbf{G}''_{+,ij}(-\nu) \tilde{R}_j'(\nu + 2\omega) \right] \right\}.\end{aligned}\quad (34)$$

When  $\nu = \omega$ , we obtain the dispersions in quadrature and the correlations to be given by

$$\begin{aligned}\sigma_{i,c}^2(\omega) &= \lim_{\Delta\nu \rightarrow 0^+} \int_{\omega-\Delta\nu}^{\omega+\Delta\nu} \langle \tilde{X}'_i(\omega) \tilde{X}'_i(\nu') \rangle d\nu' \\ &= 2\pi D \sum_j \left[ |\tilde{\mathbf{G}}_{0,ij}(\omega)|^2 + |\mathbf{G}_{+,ij}(\omega)|^2 + |\mathbf{G}_{+,ij}(-\omega)|^2 + 2 \operatorname{Re} \left\{ \tilde{\mathbf{G}}_{0,ij}(\omega) \mathbf{G}_{+,ij}(\omega) \right\} \right],\end{aligned}\quad (35)$$

$$\begin{aligned}\sigma_{i,s}^2(\omega) &= \lim_{\Delta\nu \rightarrow 0^+} \int_{\omega-\Delta\nu}^{\omega+\Delta\nu} \langle \tilde{X}''_i(\omega) \tilde{X}''_i(\nu') \rangle d\nu' \\ &= 2\pi D \sum_j \left[ |\tilde{\mathbf{G}}_{0,ij}(\omega)|^2 + |\mathbf{G}_{+,ij}(\omega)|^2 + |\mathbf{G}_{+,ij}(-\omega)|^2 - 2 \operatorname{Re} \left\{ \tilde{\mathbf{G}}_{0,ij}(\omega) \mathbf{G}_{+,ij}(\omega) \right\} \right],\end{aligned}\quad (36)$$

$$\sigma_{i,cs}(\omega) = \lim_{\Delta\nu \rightarrow 0^+} \int_{\omega-\Delta\nu}^{\omega+\Delta\nu} \langle \tilde{X}'_i(\omega) \tilde{X}''_i(\nu') \rangle d\nu' = 4\pi D \sum_j \operatorname{Im} \left\{ \tilde{\mathbf{G}}_{0,ij}(\omega) \mathbf{G}_{+,ij}(\omega) \right\}, \quad (37)$$

where we used

$$\begin{aligned}\langle \tilde{R}'_i(\nu) \tilde{R}'_j(\nu') \rangle &= 2\pi D \delta_{ij} [\delta(\nu - \nu') + \delta(\nu + \nu')], \\ \langle \tilde{R}'_i(\nu) \tilde{R}''_j(\nu') \rangle &= 0, \\ \langle \tilde{R}''_i(\nu) \tilde{R}''_j(\nu') \rangle &= 2\pi D \delta_{ij} [\delta(\nu - \nu') - \delta(\nu + \nu')].\end{aligned}\quad (38)$$

The most general case of dispersions where we take into account all the cross correlations is given by

$$\begin{aligned}\sigma_{ij,c}^2(\omega) &= \lim_{\Delta\nu \rightarrow 0^+} \int_{\omega-\Delta\nu}^{\omega+\Delta\nu} \langle \tilde{X}'_i(\omega) \tilde{X}'_j(\nu') \rangle d\nu' \\ &= 2\pi D \sum_k \left[ \mathbf{G}'_{0,ik}(\omega) \mathbf{G}'_{0,jk}(\omega) + \mathbf{G}''_{0,ik}(\omega) \mathbf{G}''_{0,jk}(\omega) + \mathbf{G}'_{+,ik}(\omega) \mathbf{G}'_{+,jk}(\omega) + \mathbf{G}''_{+,ik}(\omega) \mathbf{G}''_{+,jk}(\omega) \right. \\ &\quad \left. + \operatorname{Re} \left\{ \mathbf{G}_{0,ik}(\omega) \mathbf{G}_{+,jk}(\omega) + \mathbf{G}_{+,ik}(\omega) \mathbf{G}_{0,jk}(\omega) \right\} \right], \\ \sigma_{ij,s}^2(\omega) &= \lim_{\Delta\nu \rightarrow 0^+} \int_{\omega-\Delta\nu}^{\omega+\Delta\nu} \langle \tilde{X}''_i(\omega) \tilde{X}''_j(\nu') \rangle d\nu' \\ &= 2\pi D \sum_k \left[ \mathbf{G}'_{0,ik}(\omega) \mathbf{G}'_{0,jk}(\omega) + \mathbf{G}''_{0,ik}(\omega) \mathbf{G}''_{0,jk}(\omega) + \mathbf{G}'_{+,ik}(\omega) \mathbf{G}'_{+,jk}(\omega) + \mathbf{G}''_{+,ik}(\omega) \mathbf{G}''_{+,jk}(\omega) \right. \\ &\quad \left. - \operatorname{Re} \left\{ \mathbf{G}_{0,ik}(\omega) \mathbf{G}_{+,jk}(\omega) + \mathbf{G}_{+,ik}(\omega) \mathbf{G}_{0,jk}(\omega) \right\} \right], \\ \sigma_{ij,cs}(\omega) &= \lim_{\Delta\nu \rightarrow 0^+} \int_{\omega-\Delta\nu}^{\omega+\Delta\nu} \langle \tilde{X}'_i(\omega) \tilde{X}''_j(\nu') \rangle d\nu' = 2\pi D \sum_k \left\{ \mathbf{G}'_{0,ik}(\omega) \mathbf{G}''_{0,jk}(\omega) - \mathbf{G}''_{0,ik}(\omega) \mathbf{G}'_{0,jk}(\omega) \right. \\ &\quad \left. + \mathbf{G}'_{+,ik}(\omega) \mathbf{G}''_{+,jk}(\omega) - \mathbf{G}''_{+,ik}(\omega) \mathbf{G}'_{+,jk}(\omega) + \operatorname{Im} \left[ \mathbf{G}_{0,ik}(\omega) \mathbf{G}_{+,jk}(\omega) + \mathbf{G}_{+,ik}(\omega) \mathbf{G}_{0,jk}(\omega) \right] \right\}.\end{aligned}\quad (39)$$

In the Appendix B, we diagonalize the  $2N \times 2N$  covariance matrix whose entries are given above.

Based on Eq. (A13), the maximum amount of squeezing will be given by the smallest eigenvalue

of the covariance matrix.

### III. NUMERICAL RESULTS AND DISCUSSION

We plot in panel (a) of Fig. 1 the numerical data points in the  $\tilde{x}'(\omega)$ - $\tilde{x}''(\omega)$  plane with  $F_p = 0$  and in panel (b)  $F_p = 0.025$  and  $\omega = 1$ . In panels (c) and (d), we plot the histograms of the data points alongside the Gaussian distributions obtained from theory, corresponding to the results of panels (a) and (b), respectively. Each data point is a Fourier transform performed over a time series obtained from the integration of Eq. (1). The integration time step is  $dt = T/128$ , where  $T = 2\pi/\omega$ . The first  $512T$  of each time series are discarded so as transients die out and the FT is performed over a time span of further  $512T$ . There are  $N = 1000$  data points in this plot. Not only we see squeezing in the elongated shape of the cloud of data points, but we also obtain quantitative agreement in fitting the normalized histograms of the  $\tilde{x}'(\omega)$  and  $\tilde{x}''(\omega)$  data points in panel (d) with the zero-mean Gaussian distributions with dispersions given by Eqs. (17) and (18). We include the equilibrium distribution in panel (c) as a comparison. In all data presented here we used the noise level  $D = 3.08 \times 10^{-8}$  (in dimensionless units) and the quality factor  $Q = 65$ . These values were obtained from the electronic circuit implementation of a parametric oscillator given in Ref. [30]. Here, we show that the stochastic differential equations model we developed explains well the squeezing data. Rugar and Grutter [15] plotted similar results obtained experimentally, but their Gaussian distributions were only best fits from their data.

We plot in Fig. 2 the results for the dispersions in decibels relative to the dispersion at zero pump as a function of pump amplitude. One sees that the agreement between analytical (1st-order averaging approximation) as presented in Eqs. (17)-(18) and Floquet theory results from Eqs. (30)-(32) is excellent. No correlation is taken into account here. In panel (a)  $\omega = 0.999$ . As the pump amplitude  $F_p$  is increased up to the instability threshold one of the quadratures is squeezed down to a minimum above  $-6$  dB and then it starts growing again. This type of behavior was observed experimentally in [18] and in [21]. In panel (b)  $\omega = 1$ . There is a reduction of fluctuations in one quadrature and an increase of fluctuations in the other quadrature as  $F_p$  increases and one nears the instability threshold. The lower limit of deamplification reached at threshold is  $-6$  dB. There is basically no distinction between the results. In panel (c)  $\omega = 1.001$ . One sees essentially the same behavior as in panel (a). This might show that the squeezing phenomenon occurs in a very narrow frequency range around resonance, but here we are not considering the effect of

correlation as derived in Eqs. (19) and (32), where it arises with detuning even when the pump is a sine function. To obtain the Floquet exponents necessary to calculate the dispersions in this figure, we used SciPy's DOP853 ODE solver in the `solve_ivp` routine. We achieved more accurate results with this explicit Runge-Kutta integration method of 8th-order than with the RK45 ODE solver that uses an explicit Runge-Kutta method of 5(4) order.

In Fig. 3, we revisit the problem of squeezing in the single parametric oscillator, but now taking into consideration the effect of correlation. When there is correlation, the cloud of data points is no longer aligned with the  $\tilde{x}'(\omega)$  and  $\tilde{x}''(\omega)$  as shown in Fig. 1. It becomes tilted and the bivariate Gaussian distribution is no longer a product of two uncorrelated Gaussian distributions of these two statistical variates. In the Appendix we show how to transform from one bivariate Gaussian probability distribution with correlation to the diagonalized uncorrelated product of two univariate Gaussian distributions. With this diagonalized form of distribution, we obtained the width and length of the squeezed cloud. Along one principal axis, we have a dispersion  $\sigma_+^2$  and along the other we have  $\sigma_-^2$  as given in Eq. (A7) with the help of Eq. (A5). The sigmas are given by Eqs. (17)-(19) in first-order averaging and by Eqs. (30)-(32) in Floquet theory. These diagonalized dispersions are the correct measures of squeezing. One can see that the results shown in panels (b)  $\omega = 0.999$  and (c)  $\omega = 1.001$  are starkly different from the corresponding results shown in panels 2(a) and 2(c). We see here that the squeezing did not disappear as one might conclude from hastily analyzing the results of Fig. 2. In panels (a) and (d), we show that even with 10 times more detuning one can reach the  $-6$  dB lower limit of squeezing. Hence, these results show that squeezing can be far more broad band than previously thought in the literature [15, 17, 18].

In Fig. 4 we show the transition line between stable quiescent solution and unstable regions of the coupled parametric-harmonic resonators model. Along most of this transition line there is agreement between the results of harmonic balance (or averaging) and Floquet theory predictions, except at a narrow stretch near the middle where both methods predict very different lines. We tested numerically and the Floquet theory results indeed indicate the correct outcome. This region occurs when all Floquet multipliers are complex. For some reason the authors do not know yet, the harmonic balance approximation breaks down. It turns out that this region is very important for deep squeezing as we shall see next.

In Fig. 5, we show the phase sensitivity of the coupled parametric amplifier-harmonic oscillator model of Eq. (2), the linearized version of the model investigated in Refs. [21, 34]. Here,  $r_1(t) = 0$  and  $r_2(t)$  are replaced by  $\cos(\omega t + \varphi(t))$ . This is similar to the method used by Rugar and Grütter

to determine squeezing from the coherent response dependent on phase in degenerate parametric amplification. This approach is used because stochastic simulations are expensive in terms of computational resources and time. We note that this is an accurate verification of the squeezing model for the coupled resonators only if there is only one added noise input and if the detuning is very small. Here,  $\dot{\varphi} = \omega_s - \omega = 2^{-14}\omega$ , in such a way that the phase is swept almost quasi-statically, what emulates the method of Rugar and Grütter in only one integration run after the transients die out. In panel **A**, we show a long time series of  $y(t)$  divided by the amplitude of  $y(t)$  we obtain when  $F_p = 0$ . In panel **B**, we use the envelope of  $y(t)/y_0$  to obtain the gain in decibel. We obtain a deamplification around  $-33$  dB, which is a much deeper squeezing than the original results of Rugar and Grütter. Unlike previous results with deep squeezing, we did not use any feedback. When one drives only the parametric resonator, only modest squeezing above  $-6$  dB is obtained.

In Fig. 6 we show the results of squeezing for the coupled parametric-harmonic resonator model. We can see in panel **A** that very deep squeezing occurs before the onset of instability. Besides this, it has the added advantage over previous results in the literature that the deepest squeezing does not occur at the threshold of oscillations and also that the other quadrature fluctuations do not diverge as happens in the single parametric resonator. Furthermore, the heating is bounded in all channels up to the frontier of instability. This is ultimately due to the fact that all Floquet exponents are complex at the instability threshold for this choice of parameters with  $\omega = 1$ . This feature is possible in coupled parametrically-driven resonator systems whose dynamics cannot be simplified to a superposition of uncoupled normal modes. In this figure, we show results for the diagonalized dispersions which are obtained from the dispersions for each one of the four channels (cosine and sine channels of  $x$  and  $y$ ) and the correlations between the fluctuations of the cosine and sine channels for each resonator. This is because all Floquet multipliers are now real. The parameters used were taken from Singh *et al.* [21], except that we inverted the signal of the coupling parameters. No attempt was made to make a thorough investigation of parameter space. The theoretical model proposed here could be used, in principle, to quickly search for parameters that provide the highest squeezing. The utility of our model over brute numerical integration of stochastic differential equations becomes more evident when one is near the instability threshold (where squeezing is strongest), because at least one decay rate, the real part of a Floquet exponent, goes to zero. This results in very long times for transients to die off, what becomes very costly in terms of computational resources.

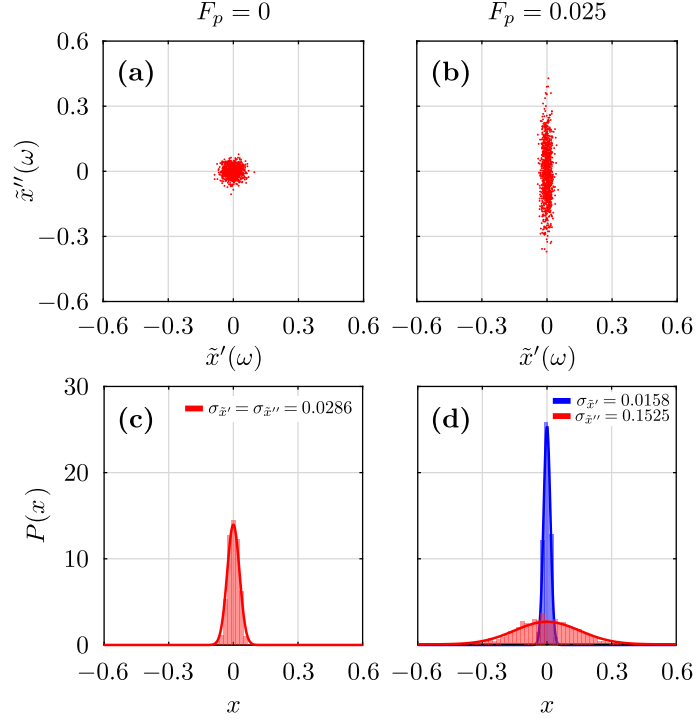


FIG. 1. In panels (a) and (b) we plot the clouds of data points of the Fourier transforms  $\tilde{x}(\omega)$ . In panel (a) we have the equilibrium cloud with no squeezing ( $F_p = 0$ ). In panel (b) we have squeezing with the pump amplitude  $F_p = 0.025$  and pump phase  $\phi_p = \pi/2$ . In all panels, we have  $Q = 65$  and  $\omega = 1$ . In panels (c) and (d), we plot the Gaussian distributions alongside the histograms for the clouds from (a) and (b) panels, respectively. In panel (c) we plot the equilibrium Gaussian distribution and in panel (d), we plot the squeezed Gaussian distributions with zero mean and dispersions given by Eq. (17) for the  $\tilde{x}'(\omega)$  data points and by Eq. (18) for the  $\tilde{x}''(\omega)$  data points.

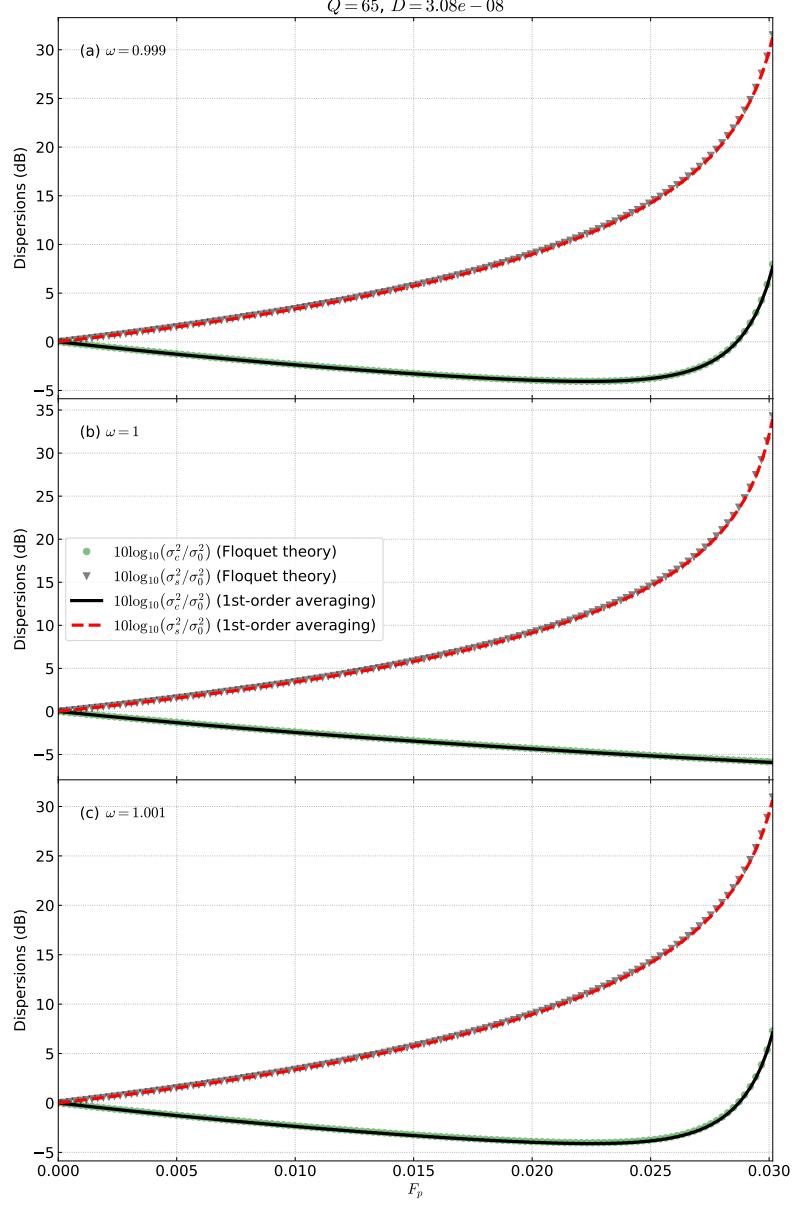


FIG. 2. Comparison of the analytical (first-order averaging) standard deviations given in Eqs. (17)-(18) of the real and imaginary parts of  $\tilde{x}(\omega)$  with the corresponding Floquet theory results given in Eqs. (30)-(31). The results are plotted in decibels relative to the equilibrium value with zero pump. In all cases  $\varphi_p = \pi/2$ . (a) At  $\omega = 0.999$ , as the pump amplitude  $F_p$  is increased up to the instability threshold, one of the quadratures is squeezed down to a minimum above  $-6$  dB and then it starts growing again. (b) At  $\omega = 1$  one sees that when the pump amplitude  $F_p$  is increased up to the instability threshold one of the quadratures is squeezed down to  $-6$  dB in amplitude while the other quadrature increases without bounds. (c) At  $\omega = 1.001$  one sees basically the same behavior as in panel (a).



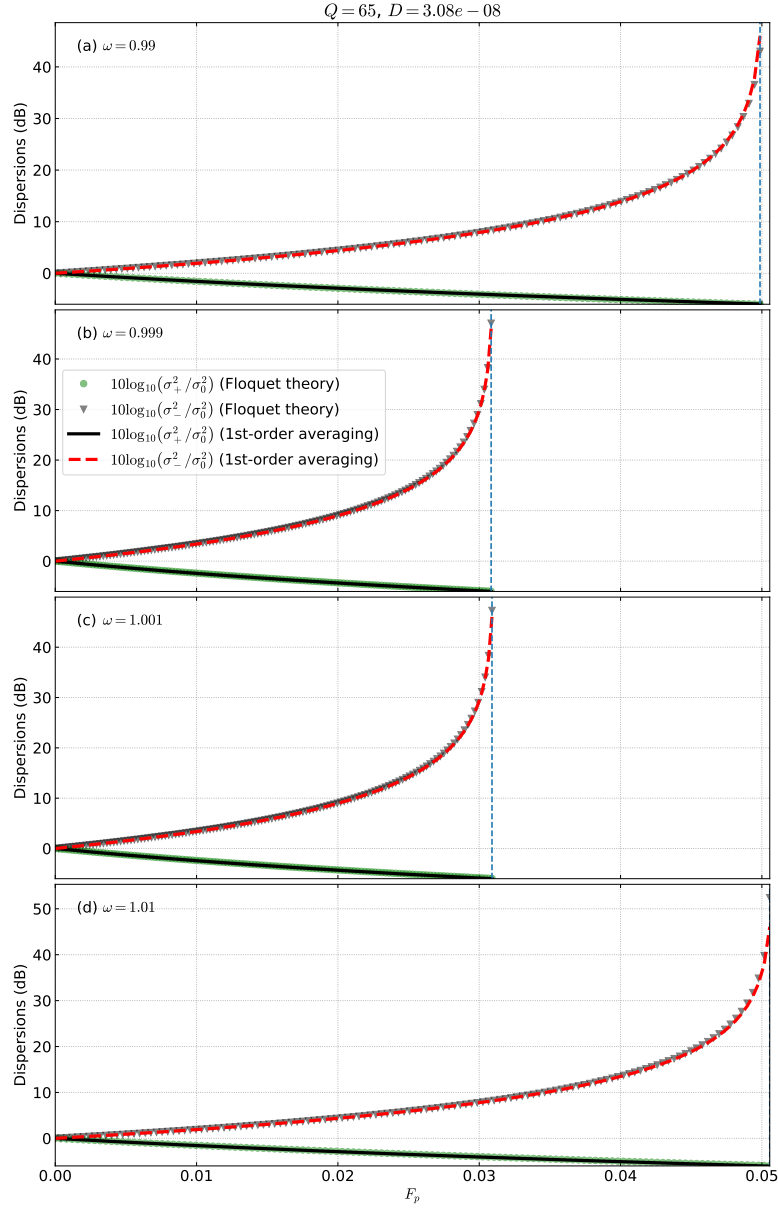


FIG. 3. Comparison of the analytical (first-order averaging) standard of the diagonalized dispersions (in the panel with no correlation) with the corresponding Floquet theory result. The diagonalization process is described in the Appendix A. In panels (a)-(d), the  $-6$  dB squeezing limit (at the bottom axes) can be reached near the instability threshold (depicted by the vertical dashed lines) even with detuning. The results for squeezing in panels (b) and (c) are in marked contrast with what happens for the same parameters in Figs. 2(a) and 2(c), respectively, where correlation was not taken into account. In panels (a) and (d) the  $-6$  dB limit can be reached even with a detuning 10 times larger than in panels (b) and (c).

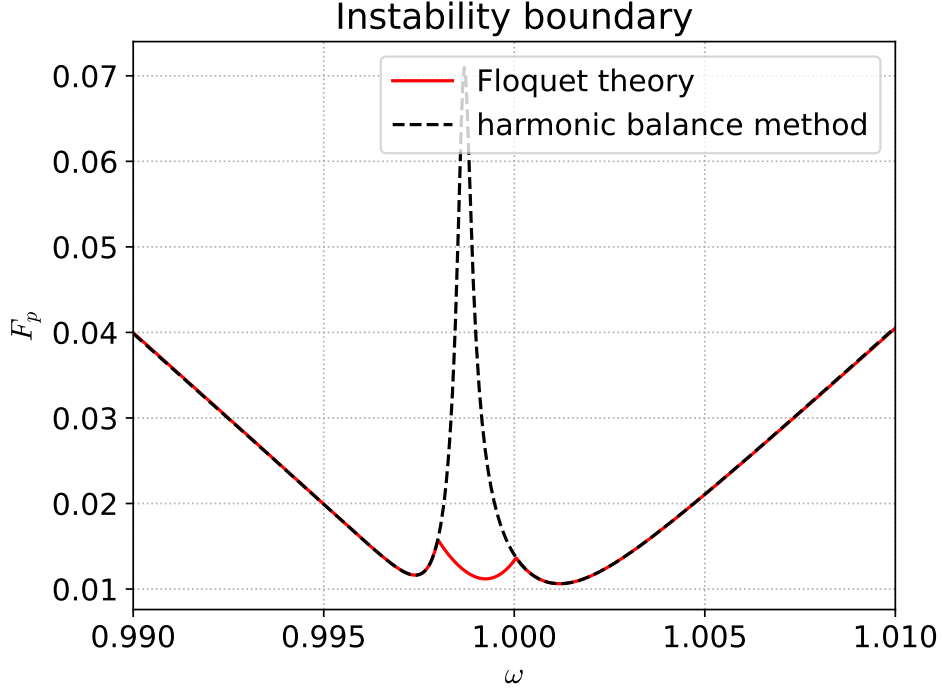


FIG. 4. Instability boundary of the parametric-harmonic coupled resonators as described in Eqs. (2) when  $r_1(t) = r_2(t) = 0$ . There is a region where the results of the harmonic balance or averaging results are very different from the boundary predicted by Floquet theory. In this region where harmonic balance breaks down all four Floquet multipliers are complex. If the dynamics could be decomposed into normal modes this result would not be possible. This is due to the constraints imposed by Liouville's formula.

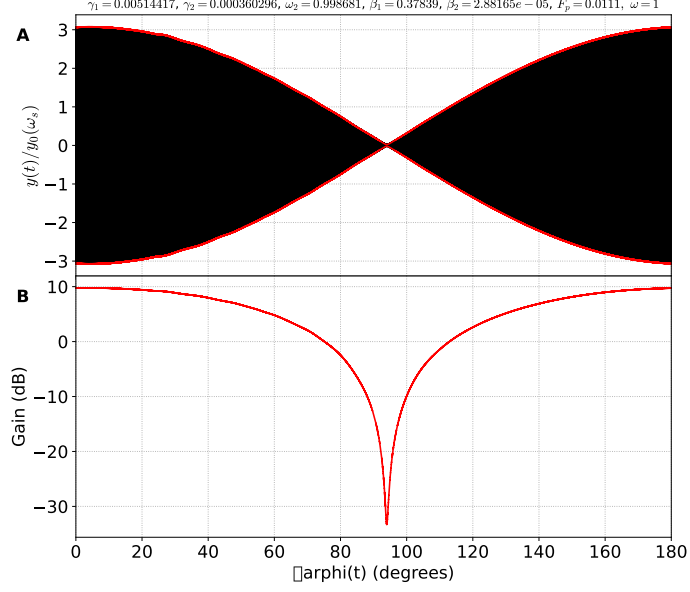


FIG. 5. Gain as a function of phase for the parametrically modulated coupled resonators described in Eq. (2), with  $r_1(t) = 0$  and  $r_2(t)$  replaced by  $\cos(\omega t + \varphi(t))$ . **A** We plot the normalized cyclo-stationary response  $y(t)/y_0$  as a function of phase  $\varphi$ , where  $y_0$  is the amplitude of oscillations of the forced harmonic resonator when  $F_p = 0$ . There is a slight detuning between  $\omega$  and  $\omega_s$  so that the phase is swept very slowly, almost quasi-statically. The envelopes are obtained from Floquet theory. **B** We use the positive envelope from **A** to obtain the gain in decibels.

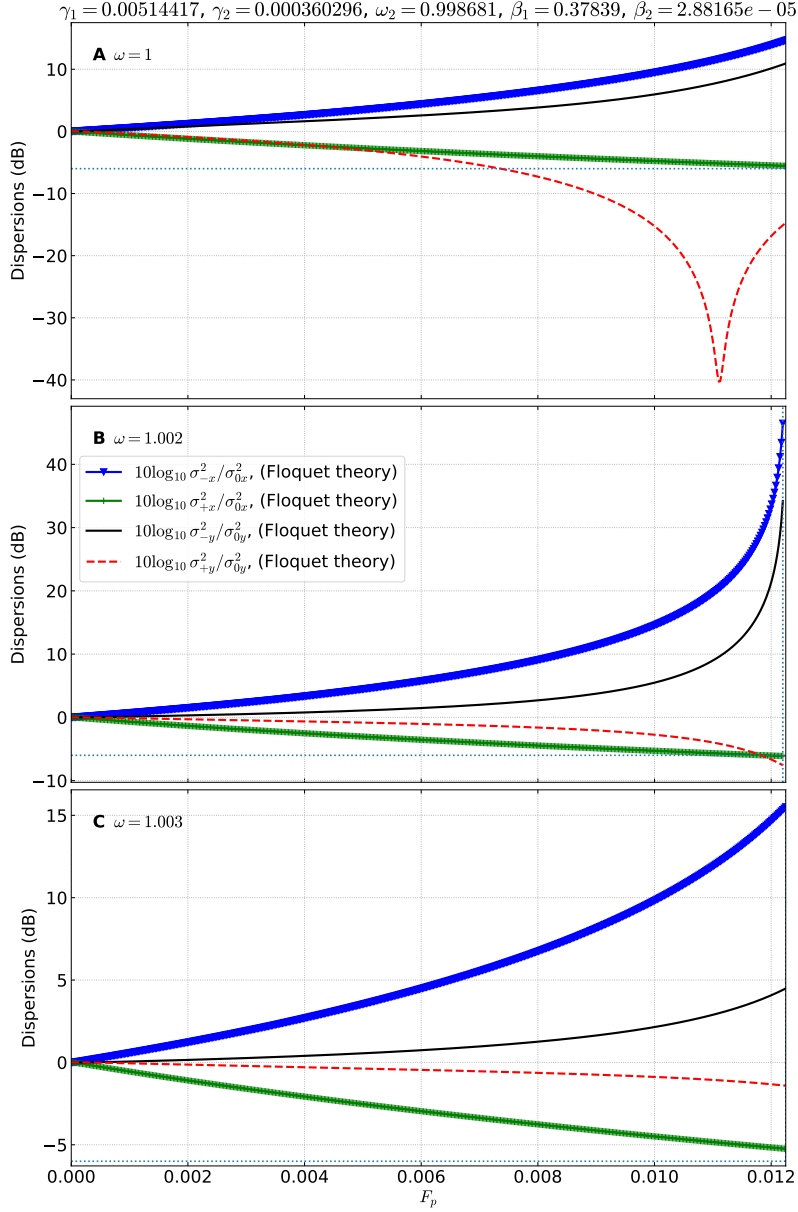


FIG. 6. Floquet theory predictions for the model given in Eq. (2). Standard deviations in decibels relative to the equilibrium values with zero pump in decibel scale. The dotted horizontal line corresponds to  $-6$  dB and the vertical dotted line the instability threshold for each case. The common parameters used in all panels are given on top of the figure. In panel (a),  $\omega = 1$ , we see that, unlike the single-degree-of-freedom parametric resonator, deep squeezing far below  $-6$  dB can be achieved in the harmonic resonator. In panel (b),  $\omega = 1.002$ , the maximum squeezing at threshold (depicted by the vertical dashed line) is slightly below  $-6$  dB. In panel (c),  $\omega = 1.003$ , one sees that even with detuning one can reach  $-6$  dB squeezing limit near the instability threshold.

#### IV. CONCLUSION

Here we developed a theoretical model based on stochastic differential equations to explain the effect of white noise squeezing that occurs in classical parametrically driven resonators with added noise. This phenomenon, which is akin to the quantum phenomenon of squeezed coherent states, was first observed in a classical micromechanical resonator in 1991 by Rugar and Grütter [15]. Unlike previous works, our results are based on the solution of stochastic differential equations both approximately, using the averaging method, and exactly, using Floquet theory. Another novelty of our model is that we obtain analytical expressions for statistical averages related to the frequency-domain response of the parametrically modulated resonator to added white noise. Each data point corresponds to a Fourier transform of a long time series with coordinates, one for each input signal in quadrature, given by the real and imaginary parts of the Fourier transform of the parametric oscillator response to the added noise. The experimental case is approximated by the ideal theoretical case in which the time constant of the LIA is infinite.

We obtained excellent agreement between the predictions of the 1st-order averaging approximations and Floquet theory near the first parametric instability when  $\omega \approx 1$  (in our dimensionless units). The strongest squeezing occurs at  $\omega = 1$  and when  $F_p$  is set at the threshold of parametric instability. While in one of the quadratures fluctuations are decreased as the pumping amplitude increases, reaching a  $-6$  dB deamplification in amplitude at the parametric instability threshold, in the other quadrature, fluctuations can increase without bounds. We showed that, unlike previously implied in the literature, squeezing does not quickly disappear with increasing (red or blue) detuning. We reached this conclusion by taking into account the effect of correlation, what to the best of our knowledge, had not been properly investigated in the literature. We believe this discovery could be relevant for the experimentalists. It is important to point out that the noise squeezing effect increases when one nears the parametric instability threshold, as can be seen in Eq. (18). We showed here that this is a feature of amplification near a period-doubling bifurcation point. It could be a generic feature of local codimension-1 bifurcation points and could occur in physical systems such as the Josephson junction amplifier [35, 36].

We developed a general model of squeezing based on Green's functions and Floquet theory that can be applied to any number of coupled parametrically modulated resonators with added noise. Here we obtained deep squeezing beyond the lower limit previously obtained in parametric systems with feedback [19, 24, 25]. We showed that the strong squeezing we found is only possible

in coupled resonators whose dynamics cannot be decomposed in normal modes. In those situations one cannot obtain deamplification below  $-6$  dB. Furthermore, it seems that strong squeezing only occurs when all Floquet multipliers are complex. We believe that our model can be applied to a wide number of parametrically-driven resonators and could be used as a guide to experimentalists in searching suitable parameter regions with deep squeezing.

The methods developed here could be applied to investigate quadrature squeezing of limit cycles of nonlinear oscillators perturbed by added noise. This could be verified experimentally in nanomechanical resonators. Also, more interestingly, since the quantum limit of these resonators has been studied in the last 10-15 years [37, 38], one could investigate what the quadrature squeezing would be in those systems. Another system of interest is the Kerr parametric oscillator which has been implemented in superconducting circuits based on Josephson junctions [39, 40]. This system is the quantum equivalent of a parametrically pumped Duffing oscillator [41]. Since networks of coupled parametrically-driven resonators (perceptrons) have been proposed as a way to implement Ising machines [42], the accurate knowledge of the threshold boundary has become a more relevant issue. Noise squeezing could play a relevant part in these systems as well. The Floquet theory method developed here could be used to obtain the instability line accurately and efficiently, and also be used to predict the amount of noise squeezing involved.

## SUPPLEMENTARY MATERIAL

The code used to generate all the numerical data and the figures of this paper is provided in the supplementary material.

## APPENDIX

### A. The Gaussian distribution with two variables

Given the Gaussian bivariate probability distribution of the type

$$P(x, y) = \frac{\sqrt{ab - c^2}}{\pi} e^{-ax^2 - by^2 - 2cxy}, \quad (\text{A1})$$

where  $a, b > 0$  and  $ab > c^2$ , we find  $\langle x \rangle = \langle y \rangle = 0$  and

$$\begin{aligned}\langle x^2 \rangle &= \frac{b}{2(ab - c^2)}, \\ \langle y^2 \rangle &= \frac{a}{2(ab - c^2)}, \\ \langle xy \rangle &= -\frac{c}{2(ab - c^2)}.\end{aligned}\tag{A2}$$

Inverting these equations, we obtain all the parameters of this distribution

$$\begin{aligned}a &= \frac{\langle y^2 \rangle}{2(\langle x^2 \rangle \langle y^2 \rangle - \langle xy \rangle^2)}, \\ b &= \frac{\langle x^2 \rangle}{2(\langle x^2 \rangle \langle y^2 \rangle - \langle xy \rangle^2)}, \\ c &= -\frac{\langle xy \rangle}{2(\langle x^2 \rangle \langle y^2 \rangle - \langle xy \rangle^2)}.\end{aligned}\tag{A3}$$

Consequently, once we have the experimental data we can find the statistical averages  $\langle x^2 \rangle$ ,  $\langle y^2 \rangle$ , and  $\langle xy \rangle$ , and from there obtain the probability distribution. We can also diagonalize the bilinear form at the exponent of the probability distribution. In other words we want to split the joint probability distribution into the product of two one variate distributions, that is  $P(x, y) = P(u, v) = P_-(u)P_+(v)$  such that  $ax^2 + by^2 + 2cxy = \lambda_- u^2 + \lambda_+ v^2$ . To achieve that, we diagonalize the following matrix

$$A = \begin{bmatrix} a & c \\ c & b \end{bmatrix}.\tag{A4}$$

The characteristic equation is  $\lambda^2 - \text{Tr } A \lambda + \det A = 0$ , from where we obtain the eigenvalues

$$\begin{aligned}\lambda_{\pm} &= \frac{\text{Tr } A \pm \sqrt{\text{Tr } A^2 - 4\det A}}{2} = \frac{a + b \pm \sqrt{(a - b)^2 + 4c^2}}{2} \\ &= \frac{\langle x^2 \rangle + \langle y^2 \rangle \pm \sqrt{(\langle x^2 \rangle - \langle y^2 \rangle)^2 + 4\langle xy \rangle^2}}{4(\langle x^2 \rangle \langle y^2 \rangle - \langle xy \rangle^2)}.\end{aligned}\tag{A5}$$

The new distribution is

$$P(u, v) = \frac{\sqrt{\lambda_- \lambda_+}}{\pi} e^{-\lambda_- u^2 - \lambda_+ v^2}\tag{A6}$$

and the new dispersions are

$$\begin{aligned}\sigma_-^2 &= \langle u^2 \rangle = \frac{1}{2\lambda_-}, \\ \sigma_+^2 &= \langle v^2 \rangle = \frac{1}{2\lambda_+}.\end{aligned}\tag{A7}$$

The normalized eigenvectors are given by

$$v_{\pm} = \frac{1}{\sqrt{1 + (\lambda_{\pm} - a)^2/c^2}} \begin{pmatrix} 1 \\ \frac{\lambda_{\pm} - a}{c} \end{pmatrix}. \quad (\text{A8})$$

$$D = \begin{pmatrix} \lambda_- & 0 \\ 0 & \lambda_+ \end{pmatrix} = S^T A S, \quad (\text{A9})$$

where

$$S = [v_- | v_+]. \quad (\text{A10})$$

We then have

$$\begin{bmatrix} u \\ v \end{bmatrix} = \begin{bmatrix} v_-^T \\ -v_+^T \end{bmatrix} \begin{bmatrix} x \\ y \end{bmatrix} \quad (\text{A11})$$

We can also assert that the tangent of the angle of the eigenvectors with respect to the  $x$  axis is given by

$$\tan \theta_{\pm} = \frac{\lambda_{\pm} - a}{c} = \frac{b - a \pm \sqrt{(b - a)^2 + 4c^2}}{2c} = \frac{\langle y^2 \rangle - \langle x^2 \rangle \mp \sqrt{(\langle x^2 \rangle - \langle y^2 \rangle)^2 + 4\langle xy \rangle^2}}{2\langle xy \rangle}. \quad (\text{A12})$$

We notice that when  $a = b$ ,  $\theta_{\pm} = \pm\pi/4$ .

## B. The Gaussian distribution with $N$ variables

Given the Gaussian  $N$ -variate probability distribution of the type

$$P(x_1, x_2, \dots, x_N) = \frac{1}{\sqrt{(2\pi)^N \det C}} e^{-\frac{1}{2} \sum_{jk} C_{jk}^{-1} x_j x_k}, \quad (\text{A13})$$

where  $A$  is a positive-defined matrix (i.e. where all eigenvalues are positive). The dispersions are given by

$$\begin{aligned} \langle x_i x_j \rangle &= \frac{1}{\sqrt{(2\pi)^N \det C}} \int_{-\infty}^{\infty} \dots \int_{-\infty}^{\infty} x_i x_j e^{-\frac{1}{2} \sum_{jk} C_{jk}^{-1} x_j x_k} dx_1 \dots dx_N \\ &= \frac{1}{\sqrt{(2\pi)^N \det C}} \frac{\partial^2}{\partial \lambda_i \partial \lambda_j} \int_{-\infty}^{\infty} \dots \int_{-\infty}^{\infty} e^{-\frac{1}{2} \sum_{jk} C_{jk}^{-1} x_j x_k + \sum_k \lambda_k x_k} dx_1 \dots dx_N \Big|_{\lambda_1 = \dots = \lambda_N = 0} \\ &= \frac{\partial^2}{\partial \lambda_i \partial \lambda_j} e^{\frac{1}{2} \sum_{jk} C_{jk} \lambda_j \lambda_k} \Big|_{\lambda_1 = \dots = \lambda_N = 0} = C_{ij} \end{aligned} \quad (\text{A14})$$



In order to obtain this result, we made the following change of coordinates  $x_j = y_j + \alpha_j$ . Thus, the exponent of the distribution from (A13) becomes

$$\begin{aligned} S &= -\frac{1}{2} \sum_{jk} C_{jk}^{-1} x_j x_k + \sum_k \lambda_k x_k = -\frac{1}{2} \sum_{jk} C_{jk}^{-1} (y_j + \alpha_j)(y_k + \alpha_k) + \sum_k \lambda_k (y_k + \alpha_k) \\ &= -\frac{1}{2} \sum_{jk} C_{jk}^{-1} y_j y_k - \sum_j \left[ \sum_k C_{jk}^{-1} \alpha_k - \lambda_j \right] y_j - \frac{1}{2} \sum_{jk} C_{jk}^{-1} \alpha_j \alpha_k + \sum_k \lambda_k \alpha_k. \end{aligned}$$

The  $\alpha_j$  are chosen such that

$$\sum_k C_{jk}^{-1} \alpha_k - \lambda_j = 0 \implies \boldsymbol{\alpha} = \mathbf{C} \boldsymbol{\lambda}$$

We obtain then

$$S = -\frac{1}{2} \sum_{jk} C_{jk}^{-1} y_j y_k + \frac{1}{2} \sum_k \lambda_k \alpha_k = -\frac{1}{2} \sum_{jk} C_{jk}^{-1} y_j y_k + \frac{1}{2} \sum_{jk} C_{jk} \lambda_k \lambda_j.$$


---

- [1] R. B. Karabalin, P. X. Feng, and M. L. Roukes, *Nano Letters* **9**, 3116 (2009).
- [2] O. Thomas, F. Mathieu, W. Mansfield, C. Huang, S. Trolhier-Mckinstry, and L. Nicu, *Appl. Phys. Lett.* **102**, 163504 (2013).
- [3] G. Prakash, A. Raman, J. Rhoads, and R. G. Reifenberger, *Review of Scientific Instruments* **83**, 065109 (2012).
- [4] S. He, N. Chen, H. Li, X. Fan, W. Dong, J. Dong, H. Zhou, X. Zhang, and J. Xu, *IEEE Photonics Journal* (2023).
- [5] M. Castellanos-Beltran, K. Irwin, G. Hilton, L. Vale, and K. Lehnert, *Nature Physics* **4**, 929 (2008).
- [6] B. H. Eom, P. K. Day, H. G. LeDuc, and J. Zmuidzinas, *Nature Phys.* **8**, 623 (2012).
- [7] M. Moreno-Moreno, A. Raman, J. Gomez-Herrero, and R. Reifenberger, *Appl. Phys. Lett.* **88**, 193108 (2006).
- [8] W. Paul, *Rev. of Mod. Phys.* **62**, 531 (1990).
- [9] J. M. L. Miller, A. Ansari, D. B. Heinz, Y. Chen, I. B. Flader, D. D. Shin, L. G. Villanueva, and T. W. Kenny, *Applied Physics Reviews* **5** (2018), doi.org/10.1063/1.5027850.
- [10] J. Lee, S. W. Shaw, and P. X.-L. Feng, *Applied Physics Reviews* **9** (2022).
- [11] A. Szorkovszky, G. A. Brawley, A. C. Doherty, and W. P. Bowen, *Phys. Rev. Lett.* **110**, 184301 (2013).
- [12] H. J. Kimble, Y. Levin, A. B. Matsko, K. S. Thorne, and S. P. Vyatchanin, *Phys. Rev. D* **65**, 022002 (2001).

- [13] Y. Chen, Journal of Physics B: Atomic, Molecular and Optical Physics **46**, 104001 (2013).
- [14] B. P. Abbott, R. Abbott, T. Abbott, M. Abernathy, F. Acernese, K. Ackley, C. Adams, T. Adams, P. Addesso, R. Adhikari, *et al.*, **Phys. Rev. Lett.** **116**, 061102 (2016).
- [15] D. Rugar and P. Grütter, **Phys. Rev. Lett.** **67**, 699 (1991).
- [16] F. DiFilippo, V. Natarajan, K. R. Boyce, and D. E. Pritchard, **Phys. Rev. Lett.** **68**, 2859 (1992).
- [17] A. N. Cleland, New Journal of Physics **7**, 235 (2005).
- [18] I. Mahboob, H. Okamoto, K. Onomitsu, and H. Yamaguchi, **Phys. Rev. Lett.** **113**, 167203 (2014).
- [19] Y. Patil, S. Chakram, L. Chang, and M. Vengalattore, **Phys. Rev. Lett.** **115**, 017202 (2015).
- [20] A. Pontin, M. Bonaldi, A. Borrielli, L. Marconi, F. Marino, G. Pandraud, G. Prodi, P. Sarro, E. Serra, and F. Marin, **Physical review letters** **116**, 103601 (2016).
- [21] R. Singh, R. J. Nicholl, K. I. Bolotin, and S. Ghosh, **Nano Letters** **18**, 6719 (2018).
- [22] Z. Zhao, H. Chen, W. Li, Z. Cheng, H. Song, Y. Wang, Q. Zhou, X. Niu, and G. Deng, in **2021 13th International Conference on Wireless Communications and Signal Processing (WCSP)** (IEEE, 2021) pp. 1–3.
- [23] A. Vinante and P. Falferi, **Phys. Rev. Lett.** **111**, 207203 (2013).
- [24] M. Poot, K. Y. Fong, and H. Tang, **New Journal of Physics** **17**, 043056 (2015).
- [25] S. Sonar, V. Fedoseev, M. J. Weaver, F. Luna, E. Vlieg, H. van der Meer, D. Bouwmeester, and W. Löffler, **Physical Review A** **98**, 013804 (2018).
- [26] R. Almog, S. Zaitsev, O. Shtempluck, and E. Buks, **Phys. Rev. Lett.** **98**, 078103 (2007).
- [27] J. S. Huber, G. Rastelli, M. J. Seitner, J. Kölbl, W. Belzig, M. I. Dykman, and E. M. Weig, **Phys. Rev. X** **10**, 021066 (2020).
- [28] K. Wiesenfeld, **J. of Stat. Phys.** **38**, 1071 (1985).
- [29] A. A. Batista, **J. of Stat. Mech. (Theory and Experiment)** **2011**, P02007 (2011).
- [30] A. A. Batista, A. A. L. de Souza, and R. S. N. Moreira, **Journal of Applied Physics** **132**, 174902 (2022).
- [31] A. A. Batista, **Phys. Rev. E** **86**, 051107 (2012).
- [32] J. M. L. Miller, D. D. Shin, H.-K. Kwon, S. W. Shaw, and T. W. Kenny, **Appl. Phys. Lett.** **117**, 033504 (2020).
- [33] A. A. Batista, **arXiv preprint arXiv:2306.13556v3** (2023).
- [34] R. Singh, A. Sarkar, C. Guria, R. J. Nicholl, S. Chakraborty, K. I. Bolotin, and S. Ghosh, **Nano Letters** **20**, 4659–4666 (2020).

- [35] T. Yamamoto, K. Inomata, M. Watanabe, K. Matsuba, T. Miyazaki, W. D. Oliver, Y. Nakamura, and J. Tsai, *Applied Physics Letters* **93**, 042510 (2008).
- [36] R. Vijay, M. H. Devoret, and I. Siddiqi, *Review of Scientific Instruments* **80**, 111101 (2009).
- [37] A. D. O’Connell, M. Hofheinz, M. Ansmann, R. C. Bialczak, M. Lenander, E. Lucero, M. Neeley, D. Sank, H. Wang, M. Weides, and A. N. Cleland, *Nature* **464**, 697 (2010).
- [38] C. Samanta, S. De Bonis, C. Møller, R. Tormo-Queralt, W. Yang, C. Urgell, B. Stamenic, B. Thibault, Y. Jin, D. Czaplewski, *et al.*, *Nature Physics* **19**, 1340–1344 (2023).
- [39] H. Goto, *Journal of the Physical Society of Japan* **88**, 061015 (2019).
- [40] A. Grimm, N. E. Frattini, S. Puri, S. O. Mundhada, S. Touzard, M. Mirrahimi, S. M. Girvin, S. Shankar, and M. H. Devoret, *Nature* **584**, 205 (2020).
- [41] A. A. Batista and A. A. Lisboa de Souza, *Jour. of Appl. Phys.* **128**, 244901 (2020).
- [42] T. L. Heugel, O. Zilberberg, C. Marty, R. Chitra, and A. Eichler, *Physical Review Research* **4** (2022), [10.1103/physrevresearch.4.013149](https://doi.org/10.1103/physrevresearch.4.013149).